A Case of Excessive Autophagocytosis with Multiorgan Involvement and Low Clinical Penetrance

Sikora J.[1], Dvořáková L.[1], Vlášková H.[1], Stolnaja L.[1], Betlach J.[2], Špaček J.[3], Elleder M.[1]

[1]Institute of Inherited Metabolic Disorders, 1st Medical Faculty, Charles University and General Teaching Hospital, Prague, Czech Republic

[2]Department of Pathology, Hospital Havlíčkův Brod, Czech Republic

[3]The Fingerland Department of Pathology, Faculty of Medicine in Hradec Králové, Charles University, Czech Republic

Summary

An autopsy and microscopic analyses of a 74-year-old female with a clinical history of cardiac hypertrophy and hypertension disclosed a pronounced distension of lysosomal compartment with signs of excessive autophagocytosis, predominantly in cardiomyocytes, hepatocytes and smooth muscle cells of the small intestine. The histological storage pattern did not correspond to the usual changes seen in defined lysosomal storage disorders. The amount of age-related lipopigment was low in all tissues. Confocal microscopy of liver tissue samples documented a progressive loss of mitochondrial epitopes in the distended lysosomal compartment along the porto-central axis of hepatic lobules. The possibility to detect subunit c of mitochondrial ATP synthase (SCMAS) indicated extensive intra-lysosomal degradation of mitochondria, both in hepatocytes and smooth muscle cells. The SCMAS epitope can thus be considered a valuable immunohistochemical marker of autophagocytic mitochondrial degradation. The distended lysosomes also displayed tissue specific ubiquitination. Absence of immuno-detectable p62 protein excluded aggresome formation. An inherent dysfunction of the late endosomal/lysosomal LAMP2 protein (Danon disease), was excluded on the basis of LAMP2 gene sequence analysis and LAMP2 protein levels. Whether the observed process reflects a primary dysregulation of the constitution of the autophagosomal membrane or was induced by defects in other cellular components, remains unanswered. Whatever mechanism involved, the findings should be considered relevant in differential diagnostics, despite their low clinical penetrance, should be registered and thus rendered available for future definition.

Key words: autophagocytosis – cardiomyopathy – hepatopathy – lysosomes - subunit C of mitochondrial ATP synthase

Souhrn

Případ excesivní autofagocytózy s multiorgánovým postižením a nízkou klinickou penetrancí

Pitva a následné histologické vyšetření u 74leté zemřelé s klinickou anamnézou hypertrofie srdeční a hypertenze odhalily významnou distenzi lysosomálního kompartmentu s rysy excesivní autofagocytózy. Změny byly nejvíce vyjádřeny v kardiomyocytech, hepatocytech a hladkých svalových buňkách tenkého střeva. Histologické změny neměly povahu jakéhokoliv z popsaných lysosomálních střádacích onemocnění a také množství lipofuscinu nebylo zvýšené v žádné z vyšetřených tkání. Vícečetná imunofluorescenční barvení a konfokální mikroskopie vzorků jaterního parenchymu odhalily progresivní degradaci mitochondriálních epitopů v postupně distendujícím lysosomálním kompartmentu s porto-centrálním gradientem. Imunohistochemická detekce podjednotky C mitochondriální ATP syntázy potvrdila intralysosomální degradaci mitochondrií jak v hepatocytech tak i v hladkých svalových buňkách tenkého střeva. S ohledem na tento nález lze imunohistochemický průkaz podjednotky c mitochondriální ATP syntázy považovat za metodu vhodnou pro detekci autofagocytární degradace mitochondrií. Distendovaný lysosomální kompartment vykazoval tkáňově specifickou ubikvitinaci, která však na základě detekce p62 proteinu nevykazovala „aggresomální" charakteristiky. Inherentní porucha pozdně endosomálního/lysosomálního LAMP2 proteinu (Danonova choroba) byla vyloučena na úrovni DNA i proteinové exprese. Zda se v tomto konkrétním případě jedná o primární poruchu konstituce autofagosomální membrány, či zda příčina tkví v jiném buněčném kompartmentu, zůstává nezodpovězeno. Přes neznalost molekulární podstaty a relativně malou klinickou penetranci by měly být tyto stavy zohledňovány v diferenciální diagnostice, registrovány a tím připravovány ke konečnému objasnění.

Klíčová slova: autofagocytóza – kardiomyopatie – hepatopatie – lysosomy – podjednotka C mitochondriální ATP syntázy

Čes.-slov. Patol., 43, 2007, No. 3, p. 93–103

Autophagocytosis represents one of the two main "bulk" degradation pathways in eukaryotic cells and is an essential part in programmed cell death (PCD) type II (4). Autophagocytosis has been repeatedly documented as a key mechanism involved in the pathogenesis of a variety of human pathological conditions, such as tumor genesis (28), neurodegeneration (17) and host-to-pathogen responses (7). Severe myopathies with autophagic features have been repeatedly described after administration of certain pharmacological agents, especially of statins (2) and colchicines (3, 14). There is a growing number of reports regarding primary vacuolar autophagocytosis related disorders (reviewed by Nishino (26)) inherited as monogenic Mendelian traits. Of these, the best defined are Danon disease (MIM 300257), an X linked dominant disorder caused by pathogenic variations in the *LAMP2* (lysosomal associated membrane protein 2) gene, dominated by skeletal and cardiac muscle affection (32), and two allelic disorders (hereditary inclusion body myopathy and distal myopathy with rimmed vacuoles) resulting from pathogenic variations in the *GNE* (UDP-N-acetylglucosamine 2-epimerase/N-acetylmannosamine kinase) gene (MIM 600737, 605820) (27).

Other autophagocytosis – related pathological entities, with prevailing skeletal muscle involvement, have only been defined at the clinical phenotype level: X-linked myopathy with excessive autophagocytosis (XMEA) associated with the accumulation of complement C5b-9 membrane attack complex (MAC) (16), infantile autophagocytic vacuolar myopathy (33), and a recently reported autophagocytic vacuolar disorder described in a pair of twin siblings (15).

In addition, there are two reports by Kaneda et al. (19) and Saijo et al. (31) describing an autophagocytic disorder with a late onset, multiorgan involvement, cardiomyopathy and elevated plasma levels of brain natriuretic peptide in one of them.

In this report we present an additional case of a 74-year-old female patient suffering from a slowly progressing multiorgan disorder, dominated by excessive autophagocytosis. The presented case belongs, in our opinion, to the group of enhanced autophagocytosis- related disorders with low clinical penetrance, and is, in many aspects, substantially different from the reports mentioned above. The results from this case also point to certain new aspects of the autophagocytosis process and ubiquitin related lysosomal degradation.

Case report

The clinical status of the patient, a 74-year-old female, while considerable, was in most aspects unremarkable and included presumed ischemic heart disease with bilateral cardiac hypertrophy, hypertension, an AV block requiring permanent cardiac stimulation, chronic bronchitis with decreased ventilation parameters, dyslipidemia (Simvacard 20 mg/day for several months prior to death), corticoid-dependent rheumatoid arthritis (Prednisone 5 mg/day for 5 years), and diabetes mellitus type II (treated by diet only). Other significant clinical conditions, except for a period of unexplained dyspepsia, were absent. The patient succumbed to progressive cardio-respiratory failure at the age of 74 years. Laboratory findings from the 5 year period prior to death revealed that blood glucose, urea and creatinine were slightly elevated, total blood cholesterol, HDL and LDL cholesterol, triacylglycerols and ApoB were within normal ranges (see above Simvacard treatment), while aminotransferases (ALT, AST), g-glutamyltransferase and creatine phosphokinase levels were slightly elevated during the three months prior to death. Other biochemical values, as well as blood count were within normal ranges.

Family history revealed that the patient's father died of a myocardial infarction at the age of 61 years and her mother died of pulmonary embolism at the age of 75 years. The patient's sister is without clinical problems. Only one of the sons agreed to undergo a detailed clinical examination, including cardiac sonography, the results of which failed to disclose any abnormalities.

Materials and methods

The autopsy did not reveal any gross macroscopic changes other than bilateral cardiac hypertrophy (540 g), signs of chronic heart failure, and multiple erosions of the gastric mucosa with terminal hemorrhage (500 ml). The spleen (210 g) showed signs of chronic venous congestion. Atherosclerosis was minimal. Standard histopathological examination disclosed abnormal vacuolar cardiomyopathy, and because of this, the case was referred to the Institute of Inherited Metabolic Disorders. Tissue samples (lung, liver, stomach, small intestine, myocardium and basal ganglia) were available as either formaldehyde fixed samples or formaldehyde fixed paraffin embedded (FFPE) tissue samples.

The primary antibodies that were used for immunohistochemistry are listed in Table 1. The appropriate DAKO Envision kits or rabbit anti-guinea pig HRP labeled antibody (DAKO, Copenhagen, Denmark) were used for the secondary detections.

The FFPE tissue samples of the patient's liver, left ventricular myocardium, and small intestine, together with age and sex matched as well as juvenile controls were processed for multiple

Table 1. Antibodies used for imunohistochemistry

Antigen (Antibody clone)	Source	Dilution	
		IH	IF
LAMP 1 (rabbit polyclonal)	kindly provided by Dr.S.Carlsson (University of Umea, Sweden)	1:200	
LAMP 2 (rabbit polyclonal)	kindly provided by Dr.S.Carlsson	1:200	1:100
cathepsin D (rabbit polyclonal)	DAKO, Copenhagen, Denmark	1:4000	
ubiquitin (rabbit polyclonal)	DAKO, Copenhagen, Denmark	1:1500	
ubiquitin (FPM1)	Novocastra, Newcastle upon Tyne, United Kingdom		1:100
prohibitin (II-14-10)	Lab Vision, Westinghouse, CA, USA	1:500	1:250
60 kD antigen of human mitochondria (113-1)	Biogenex, San Ramon, CA, USA	1:100	1:50
subunit c of mitochondrial ATP synthase (SCMAS)	kindly provided by prof. E.Kominami (Juntendo University, Tokyo, Japan)	1:200	1:100
p62 component of aggresome (guinea pig polyclonal)	Progen, Heidelberg, Germany	1:4000	
cytochrome oxidase (COX) subunit I (1D6E1A8)	Mitosciences, Eugene, Oregon, USA		1:500
cytochrome oxidase (COX) subunit IV (10G8D12C12)	Mitosciences, Eugene, Oregon, USA		1:500
protein disulfide isomerase (PDI) (1D3)	Stressgen, Victoria, Canada		1:500
LC3 (rabbit polyclonal)	MBL, Naka-ku Nagoya, Japan	1:500	

immunofluorescence labeling. The staining protocols generally followed the accepted protocols for double immunolabeling.

The primary antibodies used for immunofluorescence labeling are listed in Table 1. Secondary detections were performed using donkey anti-mouse IgG Alexa Fluor 555 antibody and goat anti-rabbit IgG Alexa Fluor 633 antibody (Invitrogen - Molecular Probes, Carlsbad, CA, USA) diluted 1:500. Liver sections were stained with anti-LAMP2 antibody in combination with the following: anti-60 kD mitochondrial antigen, anti-prohibitin, anti-COX I, anti-COX IV and anti-PDI antibodies, and anti-SCMAS which was combined with anti-60 kD mitochondrial antigen or anti-cathepsin D antibodies. Myocardial and small intestine tissue sections were stained with anti-LAMP2 antibody in combination with: anti-60 kD mitochondrial antigen and anti-PDI antibodies, and anti-SCMAS combined with anti-60 kD mitochondrial antigen antibody. Images were acquired using a Nikon Eclipse E800/TE 2000 microscope equipped with a C1/C1 *si* spectral confocal head. The images were restored based on deconvolution using a measured point spread function (PSF) and the classical maximum likelihood estimate algorithm (Huygens Professional software, SVI, Hilversum, The Netherlands). Co-localization maps (Fig. 3) using single pixel overlap coefficient values (in the range of 0-1) (23) were calculated using Huygens Professional Software.

Formaldehyde fixed samples were post-fixed with buffered 1% OsO_4 for 2 h, dehydrated and embedded in an Araldite-Epon mixture. Thin sections were double contrasted using uranyl acetate and lead nitrate. Muscularis externa samples, from the formalin fixed small intestine samples, were manually dissected using an Olympus SD30 stereomicroscope. The immunolabeling protocol of the 70 nm thick sections followed the protocol of Griffiths et al. (12). The primary anti-SCMAS antibody was diluted 1:40; the secondary goat anti-rabbit IgG antibody (Jackson ImmunoResearch, West Grove, PA, USA) was conjugated with colloidal gold (12 nm) and was diluted 1:30. Samples were observed and photographs taken using TESLA 500 electron microscope.

Genomic DNA was isolated from lung and myocardium FFPE tissue samples using heat deparaffinization, proteinase K digestion and phenol chloroform extraction. The entire coding region of the *LAMP2* gene (GenBank reference sequence NC_000023,), including the 5' and 3' untranslated regions and the intron/exon boundaries, was amplified in ten PCR products (including both variants of the alternatively spliced exon 9) and both strands of the PCR products were directly sequenced. The PCR product sizes, primers, PCR and sequencing reactions conditions, as well as all tissue staining protocols, are available on request.

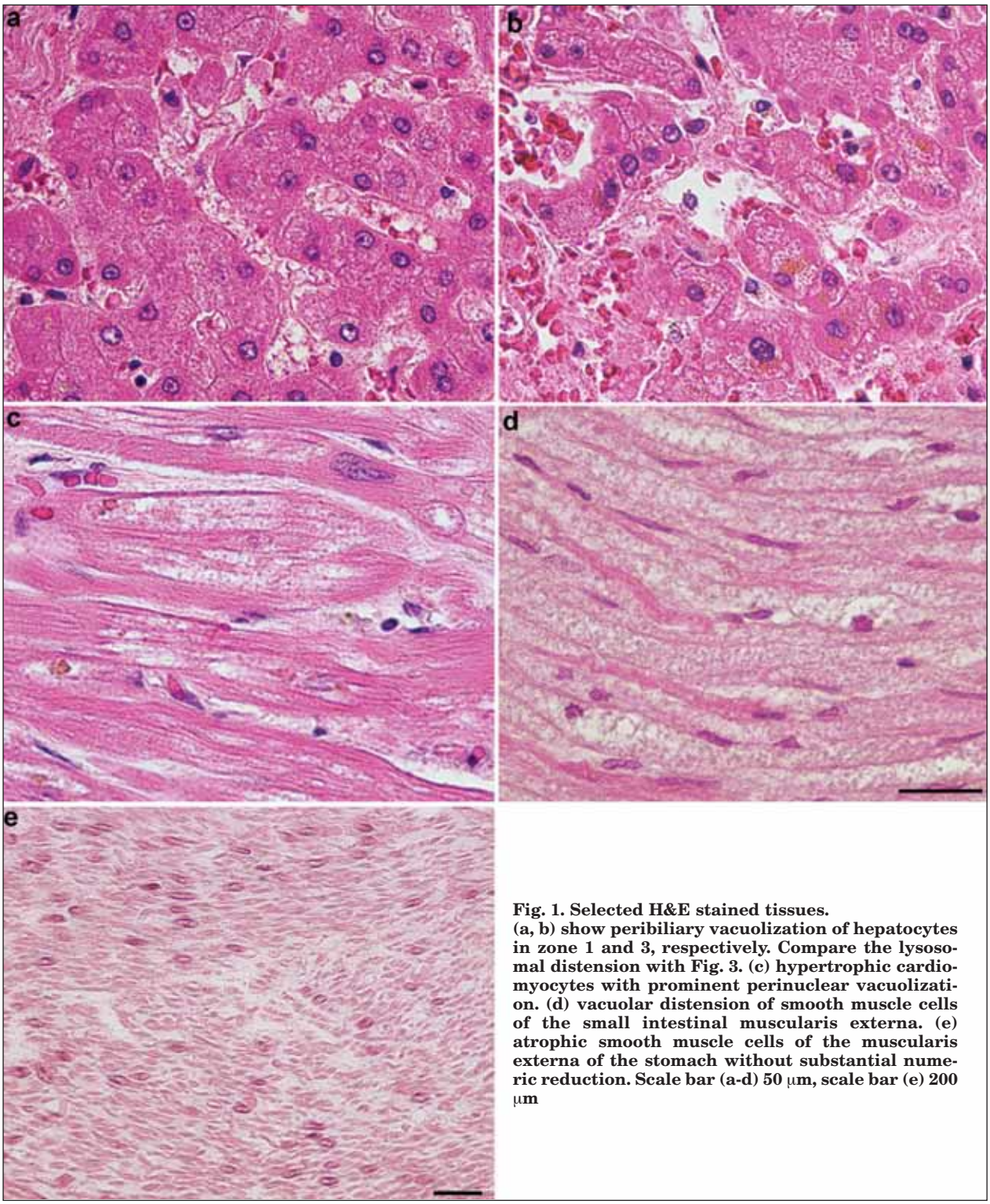

Fig. 1. Selected H&E stained tissues.
(a, b) show peribiliary vacuolization of hepatocytes in zone 1 and 3, respectively. Compare the lysosomal distension with Fig. 3. (c) hypertrophic cardiomyocytes with prominent perinuclear vacuolization. (d) vacuolar distension of smooth muscle cells of the small intestinal muscularis externa. (e) atrophic smooth muscle cells of the muscularis externa of the stomach without substantial numeric reduction. Scale bar (a-d) 50 μm, scale bar (e) 200 μm

Results

Besides the centroacinar venous congestion in the liver, there was discrete but distinct peribiliary vacuolization of zone 1 hepatocytes, which progressively increased toward zone 3, at which point, the hepatocyte cords became atrophic (Fig. 1a, b). Zone 1 hepatocytes were slightly enlarged and characterized by fine granular cytoplasm. Autofluorescent lipopigment granules were sparse and small in size and were often in the form of minivacuoles clustered within zone 3 hepatocytes. The sinusoidal CD68 positive cells showed no increase in number and showed variable, but modest, degree of cytoplasmic distension and contained small amounts of ceroid pigment.

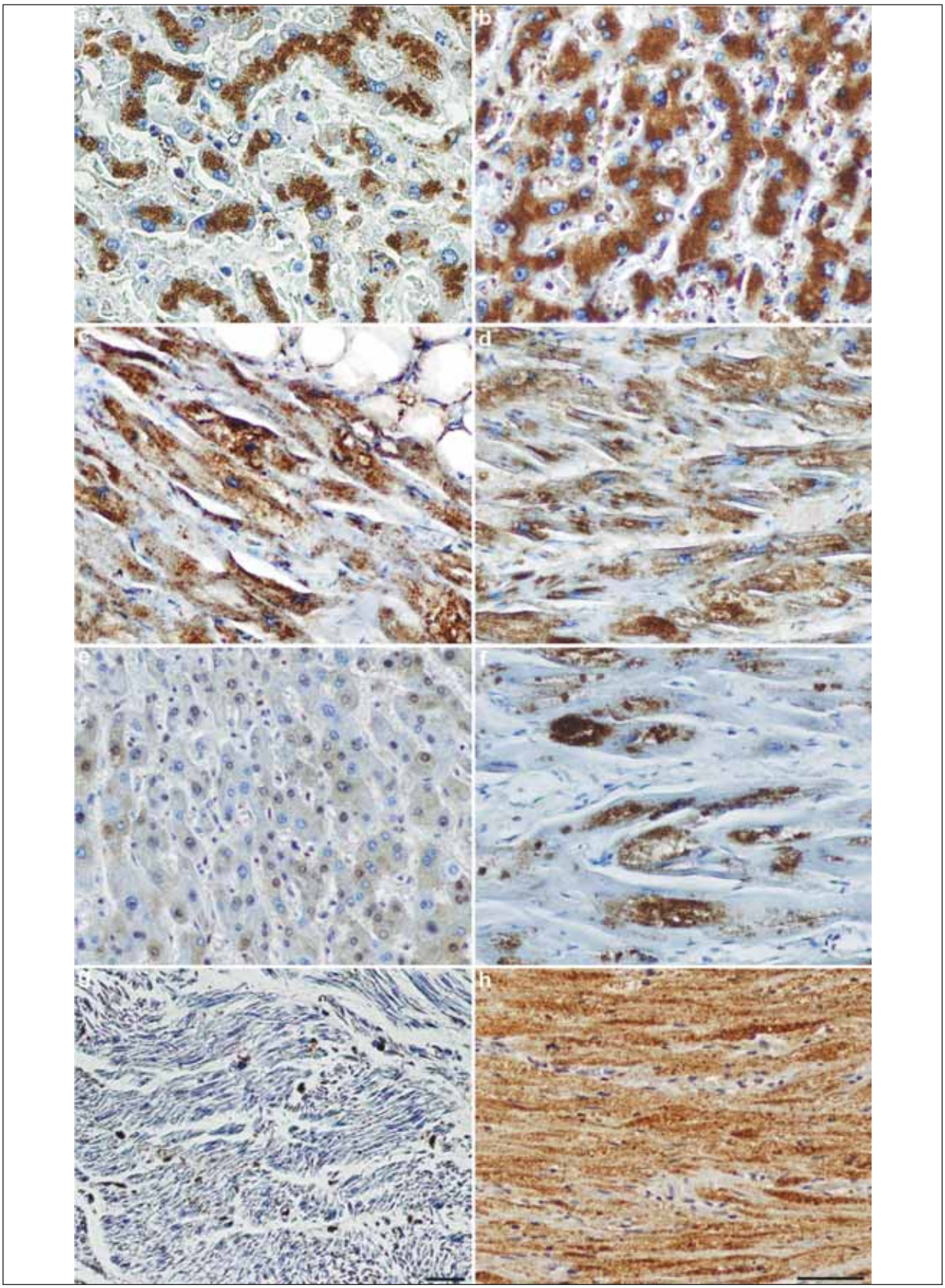

Fig. 2. Immuhistochemical detection of late endosomal/lysosomal markers and ubiquitin.
Liver sections showing distended lysosomal compartment stained for cathepsin-D (a) and LAMP2 (b). Same staining performed in myocardium, cathepsin-D (c) and LAMP2 (d). Variable extent of ubiquitin staining positivity in the liver (e), myocardium (f), atrophic gastric SMCs (g) and small intestinal SMCs (h). The ubiquitin positivity corresponds well with the distended lysosomal compartment (for comparison refer to Fig. 1). Scale bar (a-f, h) 50 μm, (g) 100 μm

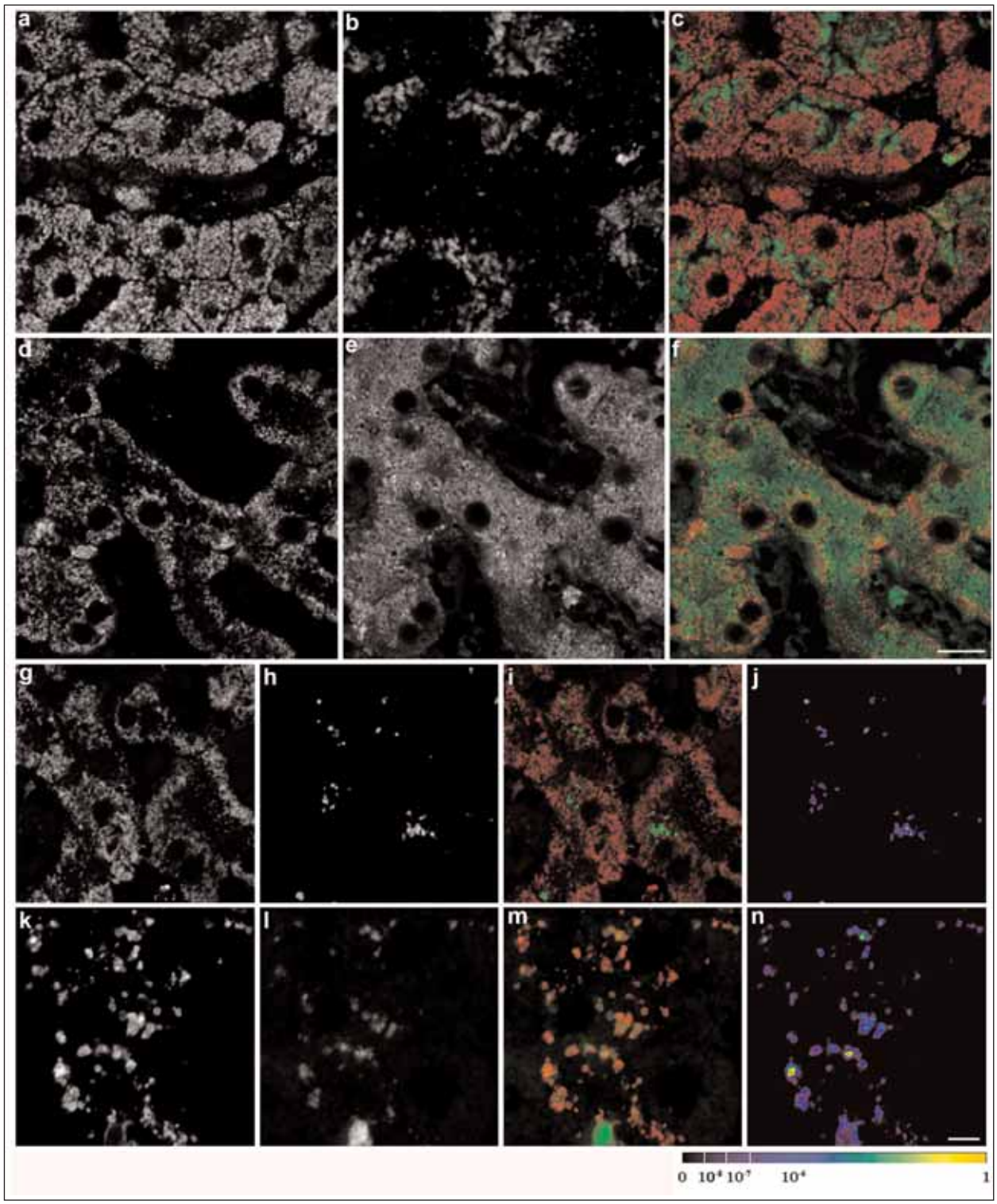

Fig. 3. Immunofluorescence and confocal laser scanning microscopy.
Zone 1 (a-c) and zone 3 (d-f) hepatocytes double labeled with LAMP 2 (b, e) antibody for late endosomal/lysosomal membranes and 60 kD mitochondrial antigen (a, d) antibody for mitochondria. Note the expansion of the late endosomal/lysosomal compartment and the parallel reduction of mitochondrial signal towards zone 3 (best documented on the merged images c, f).
(g) Shows 60 kD mitochondrial antigen antibody labeled mitochondria together with SCMAS detection (h), (i) is the merged image showing the virtual exclusion of the two signals (g, h). (k) corresponds to cathepsin D signal co-labeled with SCMAS (l), merged image (m) shows extent of co-localization of these two signals.
Panels (j, n) represent co-localization maps employing single pixel values of overlap coefficient of dual channel merged images (i, m) which were scaled with the shown LUT (beneath the panel). For the construction of the co-localization map refer to Materials and Methods. Co-localization map employing single pixel overlap coefficient values is in many ways superior to a simple RGB merge, compare (i, m) with (j, n) for the extent of the discernible signal overlap.
Scale bars (f, n) represent 10 μm

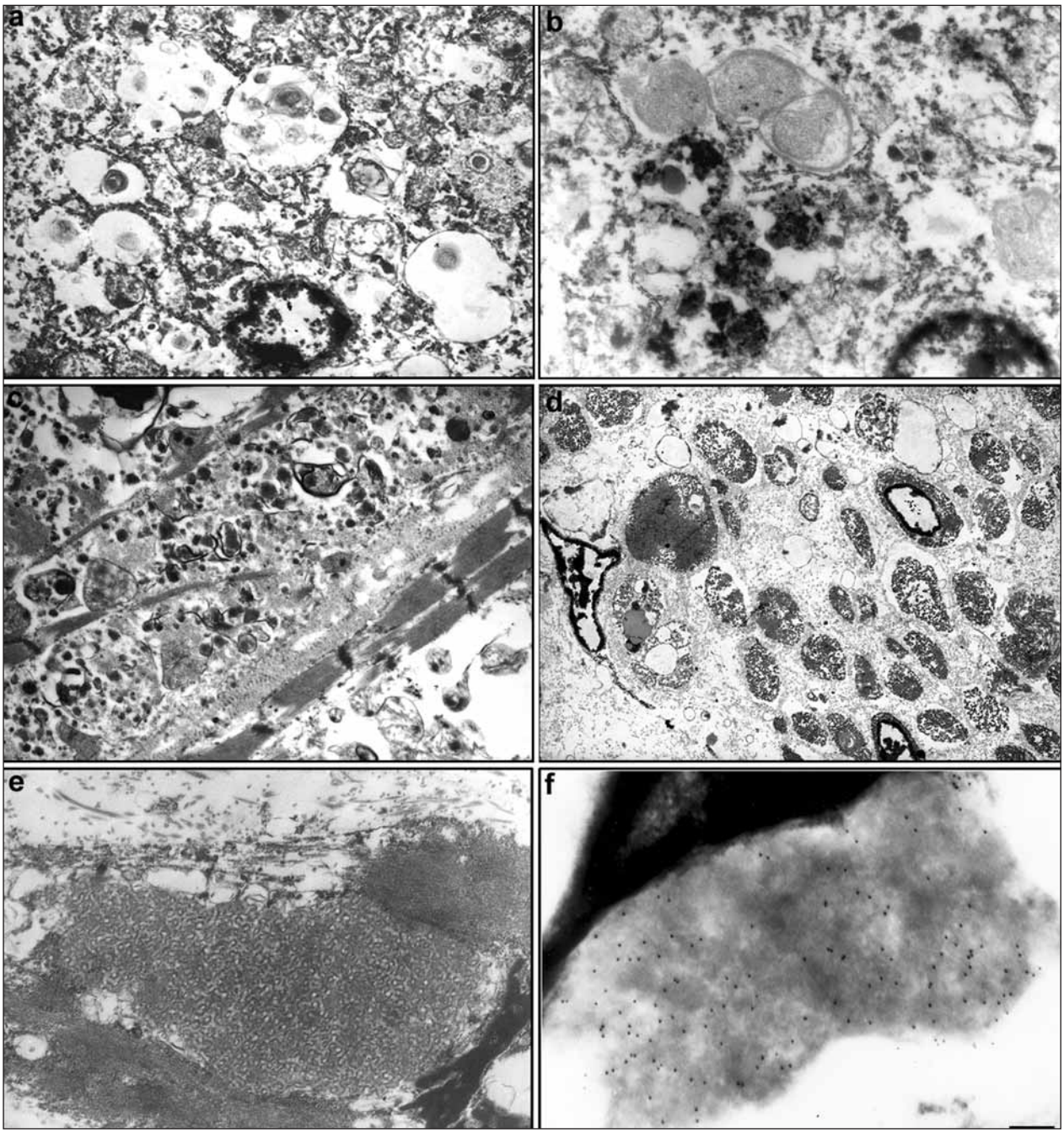

Fig. 4. Ultrastructure of the expanded lysosomal system
(a) hepatocyte lysosomes close to the centrolobular zone (zone 3), with mostly degraded content. (b) hepatocyte lysosomes close to peripheral zone (zone 1), loaded with pleomorphic content and structures strongly resembling degraded mitochondria. (c) cardiomyocyte with numerous autophagolysosomes containing degraded mitochondria. (d) smooth muscle in the small intestine, with lysosomes containing pleiomorphic material and curvilinear-like deposits shown in detail on (e). (f) immunoelectron microscopical detection of SCMAS showing a dense concentration of the epitope in curvilinear-like deposits. Magnification (a) 12 000x, (b, c) 16 000x, (d) 8 000x, (e, f) 9000x, scale bar in (f) represents 200nm.

Standard histology of the myocardium showed cardiomyocyte hypertrophy with vacuolizations of various sizes and shapes, concentrated in the perinuclear zone and containing variable amounts of autofluorescent lipofuscin (Fig. 1c). The myocardial stroma showed dispersed myofibrosis and contained a small number of CD68 positive macrophages, which exhibited variable cytoplasmic distension. Intramyocardial vessels revealed only minor abnormalities in the muscularis layer, which resembled the changes seen in the intestinal muscularis externa (see below).

The mucosa and submucosal glands of the small intestine were histologically normal. Intestinal smooth muscle cells (SMC) showed a significant degree of granulovacuolar cytoplasmic distension (Fig. 1d), with numerous,

discrete, autofluorescent granules. Peripheral autonomic neurons, in both the small intestine and stomach, were finely granular; infrequent, large axonal spheroids were observed in the intestinal mucosa and submucosa.

The ventricular mucosa had been partially altered by autolysis, but did not display any significant abnormalities. The SMCs of the intestinal muscularis externa were markedly condensed and showed signs of atrophy, but without any discernible numeric reduction (Fig. 1e).

The lung samples did not reveal any significant abnormalities; we noted scattered alveolar macrophages. The SMCs of the blood vessels and the bronchial tree did not show any significant changes.

The sample of the basal ganglia was histologically unremarkable. Neurons showed an accumulation of age related lipopigment of typical ultrastructural appearance. Axonal spheroids were present but sparse.

There was a negligible amount of birefringent liquid lipid crystals in the lysosomal compartment of any of the evaluated tissues.

With the exception of the atrophied gastric SMCs, the cytoplasmic vacuoles of all examined tissues stained intensively for the late endosomal/lysosomal membrane markers LAMP1 and 2 and with a variable intensity for the luminal lysosomal marker cathepsin D (Fig. 2 a-d).

A striking feature of the distended lysosomal compartment was its variable immunostaining positivity for ubiquitin. The lysosomal compartment of cardiomyocytes and small intestine SMCs displayed the most intensive staining with anti-ubiquitin antibody. In comparison, the distended lysosomal compartment of hepatocytes, and gastric SMCs were nearly free of ubiquitin signal (Fig. 2e-h). There was no evidence of p62 aggresomal protein accumulation in any of the ubiquitin positive tissues (myocardium, small intestine).

Staining for subunit c of mitochondrial ATP synthase (SCMAS) showed strong positivity in the lysosomes of cardiomyocytes and small intestine SMCs. The autofluorescent signal was virtually quenched after SCMAS immunohistochemical detection. This suggests that the autofluorescence originated from SCMAS deposits (data not shown). The correlation between SCMAS and lysosomal markers is discussed below.

Unfortunately, the antibody against the LC3 autophagosomal membrane component in the FFEP samples generated ambiguous results, partly because of the lack of reference samples; these results are not included in this study.

Prior to immunofluorescence labeling and laser scanning confocal imaging, the overall autofluorescence levels of the tissue sections were evaluated including the presence of age-related autofluorescent pigments. Liver samples from the patient and controls showed only a small amount of autofluorescent pigment in the peribiliary regions of zone 3 hepatocytes. Unfortunately, the prerequisites for spectral contamination could not be fulfilled in the myocardial and small intestine tissue sections.

Several criteria were evaluated in the liver tissue sections relative to the controls: (1) changes of the late endosomal/ lysosomal compartment spatially related to mitochondrial (Fig. 3 a-f) and endoplasmic reticulum (ER, data not shown) compartments in the hepatic lobule ; (2) intra-lysosomal localization of selected mitochondrial epitopes (60 kD mitochondrial antigen, prohibitin, COX I and IV) and (3) the distribution of the SCMAS signal within the tissue relative to lysosomal markers and other mitochondrial markers (Fig. 3 g-n).

LAMP 2 signal showed considerable late endosomal/lysosomal distension along the porto-central axis compared to controls. All the visualized mitochondrial epitopes showed a relatively similar staining pattern, i.e. gradual reduction of the signal towards the center of the hepatic lobule, which corresponded to late endosomal/lysosomal distension (Fig. 3 a-f). The reduction of the endoplasmic reticulum (PDI) signal towards zone 3 followed the pattern of mitochondrial epitopes (data not shown).

The confocal images were inspected for luminal entrapment of mitochondrial epitopes inside LAMP 2 positive compartment. We were not able to reliably document any of these phenomena, despite the use of deconvolution algorithms. The subresolution size of these events might be one explanation; another, and more likely, reason was the advanced state of intra-lysosomal mitochondrial epitope degradation.

To further address the issue of mitochondrial degradation, we used an antibody against SCMAS. Its detection can be considered a hallmark of mitochondrial damage or subunit c storage process, as has been shown in neuronal ceroid lipofuscinoses (NCLs) (13, 29). The presence of SCMAS signal in the peribiliary regions of hepatocytes was pronounced and again, it increased towards the center of the hepatic lobule (Fig. 3 g-n). Co-labeling with other mitochondrial markers (60 kD mitochondrial antigen) showed a virtual exclusion of the two signals, indicating the diversity of the mitochondrial population in hepatocytes; SCMAS negative/60 kD mitochondrial antigen positive (intact mitochondria) while SCMAS positive/60 kD mitochondrial antigen slightly positive or negative indicates partly or completely degraded mitochondria (Fig. 3 g-j). SCMAS epitope further resided in cathepsin D positive compartment of hepatocytes (Fig. 3 k-n), providing direct evidence of the autophagocytosis process on the optical microscopy level. Similar findings were absent in the controls samples, regardless of the labeling

combination and can hardly be assigned, as well as other described changes, to post-mortem autolysis.

Electron microscopy disclosed a wide range of changes with variable membranous ultrastructure, which often resembled the remnants of organelles, especially mitochondria, sometimes endowed with a limiting double membrane, which was highly suggestive of autophagocytic origin (Fig. 4). In hepatocytes, there was a gradual increase in electron lucent vacuoles toward the central part of the lobule (Fig. 4a), which corresponded well with optical microscopy results. Small intestinal neurons displayed an increase in mitochondria and had variable amounts of lipofuscin, as well as discrete lysosomes with a low density, amorphous content mixed with membranous structures (Fig. 4d). Small intestinal SMC deposits were highly pleiomorphic and frequentely contained a blend of curvilinear-like deposits (Fig. 4e).

Immunoelectron microscopic detection of SCMAS showed intensive staining of the curvilinear-like deposits with specific antibody (Fig. 4f).

Direct sequencing of the whole coding region of the *LAMP2* gene, did not detect any previously described or novel, potentially pathogenic sequence variations. We consider the extent of the analyzed genomic region of the *LAMP2* gene to be sufficient to exclude sequence alterations with respect to the published spectrum of sequence variations (predominance of single base substitutions or small insertions/deletions in exons or in close vicinity to exon/intron boundaries) (The Human Gene Mutation Database, http://www.hgmd.cf.ac.uk/ac). The potential effects of formaldehyde induced sequence analyses artifacts were minimized by independent PCR product pooling and repetitive independent PCR product sequencing.

Discussion

The presented case represents a late onset multiorgan disorder which manifested with features of enhanced autophagocytosis with prominent lysosomal distension in a variety of cell types, but without any signs of specific lysosomal substrate storage. The changes were most obvious in the myocardial tissue, liver tissue and SMCs of gastrointestinal tract. Unfortunately, the absence of any myopathic clinical symptoms resulted in the lack of any skeletal muscle samples for analyses. As a result, data on skeletal myopathy are limited. Optical and electron microscopy findings provided the accepted morphological hallmarks of pronounced autophagocytosis including intra-lysosomal degradation of organellar epitopes (confocal microscopy and immunoelectron microscopy).

The striking discrepancy between the intensity of the cellular pathology and its restricted clinical presentation suggests a low intensity of progression and/or the contribution of efficient compensatory mechanisms, such as hyper-regeneration (liver) or reactive compensation (cardiomyocyte hypertrophy). The nature of the disease (sporadic or hereditary) is unclear, family data does not directly support either of these possibilities, especially in light of the late age of onset, potential incomplete penetrance or possible recessive inheritance. Additional cases thus should not be ignored and care should be taken about the proper sample fixation and storage, in order to facilitate molecular analyses.

We can only speculate about the nature of the molecular mechanisms involved in the genesis of this disorder. The dominance of the autophagocytosis related changes might point to a defect in the autophagosomal/lysosomal membrane constitution machinery, associated with enhanced degradation of ubiquitin tagged moieties in autophagolysosomal compartment. However, the observed extent of ubiquitination, regardless of reason, might trigger the autophagocytic process itself, making it a secondary change (see below) (21). The presented observations of ubiquitination associated with the lysosomal compartment provide additional insight into this recently opened topic (5, 6, 24).

The autophagocytosis related disorders mentioned in the introduction, share myopathological changes in common. Most diagnostic approaches are based on descriptive microscopic methods, only LAMP-2 deficiency (Danon disease) and GNE deficiency are specified on the molecular level. We were able to narrow the differential diagnostic considerations in the described case to two potential causes: (i) LAMP2 deficiency and (ii) secondary toxic etiology related to drug administration.

(i) The ultimate argument against the diagnosis of LAMP-2 deficiency was the absence of any pathogenic sequence variation in the LAMP-2 gene. Other criteria for LAMP-2 deficiency were reported to be less specific in comparison to LAMP-2 gene DNA analysis (1, 10).

(ii) Regarding potential toxic effects, the low doses of Simvacard (simvastatin, 20 mg/day) taken by the patient do not seem to explain findings, especially since myogenic symptoms were not clinically overt. Doses of 40 mg of simvastatin per day were not able to alter ubiquinone concentrations and myopathic changes only appeared in 0.05% of patients receiving double the dose taken by our patient (2, 30). No other medications known to cause comparable adverse effects (e.g. colchicine) were present in the patient's clinical history.

The two reports on late onset multiorgan disorders with autophagocytic features (19, 31)

seem, by far, to have the most in common with the presented case, even though the clinical presentation was centered around skeletal and cardiac muscle, respectively.

We would like to make a brief comment about the possibilities of autophagocytosis detection in FFPE tissues. So far, the standard method for the detection of autophagocytosis has been the electron microscopy. While there are other methods, which are based on biochemical and dynamic cellular assays(25), these are fundamentally unsuitable for FFPE material, similarly as immunohistochemical detection of the specific marker of autophagolysosomal membrane (LC3 protein) (22). We therefore considered and demonstrated the usefulness of the antibody against subunit c of mitochondrial ATP synthase (SCMAS). SCMAS has been previously shown to accumulate, predominantly, in neuronal ceroid lipofuscinoses (13, 29) or in chloroquine intoxication (11). The genesis of SCMAS deposits in NCL has not, so far, been explained completely, but autophagocytosis has been proposed as one of the mechanisms involved in their formation (20). It is worth mentioning, that the curvilinear-like aggregates described in this case, resemble the SCMAS rich lysosomal deposits seen in many types of NCL (8, 9). The organellar selectivity of the degradative process (5, 20) can only be assessed to a limited extent.

We are convinced that conditions similar to the presented case may be under- diagnosed in routine autopsies. Even though the number of reports describing similar conditions in advanced age is still low, they should not be ignored in differential diagnostics. Careful analysis of a larger spectrum of postmortem samples including those properly fixed and stored for biochemical and molecular examination is essential to increase our knowledge of the molecular basis of these entities and of the underlying processes at the cell pathology level.

Acknowledgements

This work was supported by research project 0021620806 of the Ministry of Education, Youth and Sports of the Czech Republic.

The authors would like to thank Zdeněk Kostrouch, M.D., Ph.D. for assistance with immunoelectron microscopy, professor Ivo Šteiner M.D., Ph.D. (The Fingerland Department of Pathology, Faculty of Medicine in Hradec Králové, Charles University) for providing the patient's samples, and Mrs. Marie Kolářová and Mr. Filip Linx for technical assistance.

References

1. **Arad, M., Maron, B.J., Gorham, J.M., Johnson, W.H., Jr., Saul, J.P., Perez-Atayde, A.R. et al.:** Glycogen storage diseases presenting as hypertrophic cardiomyopathy. N Engl J Med, 352, 2005, s. 362-372.
2. **Baker, S.K.:** Molecular clues into the pathogenesis of statin-mediated muscle toxicity. Muscle Nerve, 31, 2005, s. 572-580.
3. **Baker, S.K., Goodwin, S., Sur, M., Tarnopolsky, M.A.:** Cytoskeletal myotoxicity from simvastatin and colchicine. Muscle Nerve, 30, 2004, s. 799-802.
4. **Bursch, W., Ellinger, A., Gerner, C., Frohwein, U., Schulte-Hermann, R.:** Programmed cell death (PCD). Apoptosis, autophagic PCD, or others? Ann N Y Acad Sci, 926, 2000, s. 1-12.
5. **Davis, W.L., Jacoby, B.H., Goodman, D.B.:** Immunolocalization of ubiquitin in degenerating insect flight muscle. Histochem J, 26, 1994, s. 298-305.
6. **Dickson, D.W., Wertkin, A., Kress, Y., Ksiezak-Reding, H., Yen, S.H.:** Ubiquitin immunoreactive structures in normal human brains. Distribution and developmental aspects. Lab Invest, 63, 1990, s. 87-99.
7. **Dorn, B.R., Dunn, W.A., Jr., Progulske-Fox, A.:** Bacterial interactions with the autophagic pathway. Cell Microbiol, 4, 2002, s. 1-10.
8. **Elleder, M., Lake, B.D., Goebel, H.H., Rapola, J., Haltia, M., Carpenter, S.:** Definitions of the ultrastructural patterns found in NCL. In: Goebel, H.H., Mole, S.E. Lake, B.D., ed. The neuronal ceroid lipofuscinosis (Batten disease). Amsterdam, IOS Press: 1999, 5-15.
9. **Elleder, M., Sokolova, J., Hrebicek, M.:** Follow-up study of subunit c of mitochondrial ATP synthase (SCMAS) in Batten disease and in unrelated lysosomal disorders. Acta Neuropathol (Berl), 93, 1997, s. 379-390.
10. **Fanin, M., Nascimbeni, A.C., Fulizio, L., Spinazzi, M., Melacini, P., Angelini, C.:** Generalized lysosome-associated membrane protein-2 defect explains multisystem clinical involvement and allows leukocyte diagnostic screening in Danon disease. Am J Pathol, 168, 2006, s. 1309-1320.
11. **Goebel, H.H., Kominami, E., Neuen-Jacob, E., Wheeler, R.B.:** Morphological studies on CLN2. Eur J Paediatr Neurol, 5 Suppl A, 2001, s. 203-207.
12. **Griffiths, G., Simons, K., Warren, G., Tokuyasu, K.T.:** Immunoelectron microscopy using thin, frozen sections: application to studies of the intracellular transport of Semliki Forest virus spike glycoproteins. Methods Enzymol, 96, 1983, s. 466-485.
13. **Hall, N.A., Lake, B.D., Dewji, N.N., Patrick, A.D.:** Lysosomal storage of subunit c of mitochondrial ATP synthase in Batten's disease (ceroid-lipofuscinosis). Biochem J, 275 (Pt 1), 1991, s. 269-272.
14. **Himmelmann, F., Schroder, J.M.:** Colchicine myopathy in a case of familial Mediterranean fever: immunohistochemical and ultrastructural study of accumulated tubulin-immunoreactive material. Acta Neuropathol (Berl), 83, 1992, s. 440-444.
15. **Holton, J.L., Beesley, C., Jackson, M., Venner, K., Bhardwaj, N., Winchester, B. et al.:** Autophagic vacuolar myopathy in twin girls. Neuropathol Appl Neurobiol, 32, 2006, s. 253-259.
16. **Chabrol, B., Figarella-Branger, D., Coquet, M., Mancini, J., Fontan, D., Pedespan, J.M. et al.:** X-linked myopathy with excessive autophagy: a clinicopathological study of five new families. Neuromuscul Disord, 11, 2001, s. 376-388.
17. **Jellinger, K.A., Stadelmann, C.:** Mechanisms of cell death in neurodegenerative disorders. J Neural Transm Suppl, 59, 2000, s. 95-114.
18. **Kabeya, Y., Mizushima, N., Ueno, T., Yamamoto, A., Kirisako, T., Noda, T. et al.:** LC3, a mammalian homologue of yeast Apg8p, is localized in autophagosome membranes after processing. Embo J, 19, 2000, s. 5720-5728.
19. **Kaneda, D., Sugie, K., Yamamoto, A., Matsumoto, H., Kato, T., Nonaka, I. et al.:** A novel form of autophagic vacuolar myopathy with late-onset and multiorgan involvement. Neurology, 61, 2003, s. 128-131.

20. **Koike, M., Shibata, M., Waguri, S., Yoshimura, K., Tanida, I., Kominami, E. et al.:** Participation of autophagy in storage of lysosomes in neurons from mouse models of neuronal ceroid-lipofuscinoses (Batten disease). Am J Pathol, 167, 2005, s. 1713-1728.
21. **Komatsu, M., Waguri, S., Ueno, T., Iwata, J., Murata, S., Tanida, I. et al.:** Impairment of starvation-induced and constitutive autophagy in Atg7-deficient mice. J Cell Biol, 169, 2005, s. 425-434.
22. **Kominami, E., Ezaki, J., Muno, D., Ishido, K., Ueno, T., Wolfe, L.S.:** Specific storage of subunit c of mitochondrial ATP synthase in lysosomes of neuronal ceroid lipofuscinosis (Batten's disease). J Biochem (Tokyo), 111, 1992, s. 278-282.
23. **Manders, E.M.M., Verbeek, F.J., Aten, J.A.:** Measurement of Colocalization of Objects in Dual-Color Confocal Images. Journal of Microscopy-Oxford, 169, 1993, s. 375-382.
24. **Migheli, A., Attanasio, A., Pezzulo, T., Gullotta, F., Giordana, M.T., Schiffer, D.:** Age-related ubiquitin deposits in dystrophic neurites: an immunoelectron microscopic study. Neuropathol Appl Neurobiol, 18, 1992, s. 3-11.
25. **Mizushima, N.:** Methods for monitoring autophagy. Int J Biochem Cell Biol, 36, 2004, s. 2491-2502.
26. **Nishino, I.:** Autophagic vacuolar myopathies. Curr Neurol Neurosci Rep, 3, 2003, s. 64-69.
27. **Nonaka, I., Noguchi, S., Nishino, I.:** Distal myopathy with rimmed vacuoles and hereditary inclusion body myopathy. Curr Neurol Neurosci Rep, 5, 2005, s. 61-65.
28. **Ogier-Denis, E., Codogno, P.:** Autophagy: a barrier or an adaptive response to cancer. Biochim Biophys Acta, 1603, 2003, s. 113-128.
29. **Palmer, D.N., Fearnley, I.M., Walker, J.E., Hall, N.A., Lake, B.D., Wolfe, L.S. et al.:** Mitochondrial ATP synthase subunit c storage in the ceroid-lipofuscinoses (Batten disease). Am J Med Genet, 42, 1992, s. 561-567.
30. **Rosenson, R.S.:** Current overview of statin-induced myopathy. Am J Med, 116, 2004, s. 408-416.
31. **Saijo, M., Takemura, G., Koda, M., Okada, H., Miyata, S., Ohno, Y. et al.:** Cardiomyopathy with prominent autophagic degeneration, accompanied by an elevated plasma brain natriuretic peptide level despite the lack of overt heart failure. Intern Med, 43, 2004, s. 700-703.
32. **Sugie, K., Yamamoto, A., Murayama, K., Oh, S.J., Takahashi, M., Mora, M. et al.:** Clinicopathological features of genetically confirmed Danon disease. Neurology, 58, 2002, s. 1773-1778.
33. **Yamamoto, A., Morisawa, Y., Verloes, A., Murakami, N., Hirano, M., Nonaka, I. et al.:** Infantile autophagic vacuolar myopathy is distinct from Danon disease. Neurology, 57, 2001, s. 903-905.

Address for correspondence:
Prof. M. Elleder MD, PhD
Institute of Inherited Metabolic Disorders, 1st Medical Faculty, Charles University and General Teaching Hospital, Ke Karlovu 2, Prague 2, 128 08, Czech Republic, phone: +420-2-24918283, fax: +420-2-249167119
e-mail: melleder@beba.cesnet.cz

Pleomorfní epiteloidní a světlobuněčný maligní tumor dělohy s myoidní a melanocytární diferenciací - leiomyosarkom nebo PECom? Kazuistika a přehled literatury

Kinkor Z.[1], Hes O.[2]
[1]Bioptická laboratoř, s.r.o., Plzeň
[2]Šiklův ústav patologie, LF UK, Plzeň

Souhrn

Popisován je případ třicetileté ženy operované pro náhlou příhodu břišní s obrazem krvácení do malé pánve. Nalezen byl solitární, 3 cm veliký, rozpadající se, prokrvácený tumor v děložním rohu infiltrující myometrium a nesouvisející s endometriem. Histologicky se jednalo o solidně uspořádaný nádor tvořený velkými epiteloidními elementy s hojnou oxyfilní, jemně zrnitou cytoplazmou s ložiskovou výraznou světlobuněčnou přeměnou. Nádorové buňky se vyznačovaly zjevnými jadernými nepravidelnostmi, bohatou atypickou mitotickou aktivitou a disperzně byly rozptýleny obrovské pleomorfní elementy s hyperchromními, monstrózními jádry. Komplexní imunohistochemický profil zahrnoval difúzní a homogenní expresi vimentinu, hladkosvalového aktinu, desminu, HMB45, Melan A, CD10 a EMA. U nemocné nebyla zjištěna stigmata tuberózní sklerózy a po prodělané chemoterapii je 5 měsíců bez známek progrese onemocnění. Léze byla s neurčitostí interpretována jako pleomorfní leiomyosarkom dělohy s alternativním pojmenováním maligní PECom. Vyjádřeny jsou rozpaky nad označením tumorů se smíšeným myoidním a melanocytárním fenotypem umístěných v děloze. Předkládán je přehled literatury a diskutována diferenciální diagnostika.

Klíčová slova: děloha – melanocytární diferenciace – epiteloidní/pleomorfní leiomyosarkom – angiomyolipom – PECom